

LRP 413/90

September 1990

Contributed Papers  
presented at the  
16th Symposium on Fusion Technology  
London, Great Britain, September 1990

by the TCA and TCV Groups

## TABLE OF CONTENT

<u>TCA Tokamak</u>	<u>Page</u>
- 39 GHz ECRH System for Breakdown Studies on the TCA Tokamak	01
<i>A. Pochelon, T. Goodman, D. Whaley, M.Q. Tran, A. Perrenoud, D. Reinhard, B. Jödicke, H.-G. Mathews, W. Kasparek, M. Thumm</i>	
<u>TCV Tokamak</u>	
- Design of the TCV Tokamak	07
<i>G. Tonetti, A. Heym, F. Hofmann, C. Hollenstein, J. Koechli, K. Lahlou, J.B. Lister, Ph. Marmillod, J.M. Mayor, J.C. Magnin, F. Marcus, R. Rage</i>	
- Distributed Control of the TCV Tokamak and Modular Bitbus Nodes	13
<i>J.B. Lister, Ph. Marmillod, P.F. Isoz, I.E. Placentini, B. Marletaz</i>	
- A Hybrid Matrix Multiplier for Control of the TCV Tokamak	17
<i>P.F. Isoz, J.B. Lister, Ph. Marmillod</i>	
- 19 Rectifiers to Supply the Coils of the TCV Tokamak	21
<i>D. Fasel, G. Depréville, A. Favre, J.-D. Pahuud, A. Perez, F. Puchar</i>	

## 39GHZ ECRH SYSTEM FOR BREAKDOWN STUDIES ON THE TCA TOKAMAK

A. Pochelon, T. Goodman, D. Whaley, M.Q. Tran, A. Perrenoud\*, D. Reinhard, B. Jödicke\*\*, H. G. Mathews\*\*, W. Kasperek\*\*\*, M. Thumm\*\*\*

Centre de Recherches en Physique des Plasmas, EPFL, 21, Av. des Bains, CH-1007 Lausanne, Switzerland

The design, construction and first operation of a 39GHz ECRH system (300 kW, 100ms) for low loop-voltage breakdown and startup-assist experiments on the TCA tokamak is described.

### 1. INTRODUCTION

In future large devices such as ITER, the achievable inductive electric field is limited to 0.3V/m. In the TCV tokamak under construction, the thick continuous vacuum vessel will impede purely inductive breakdown at low electric fields. Breakdown can be assured by application of ECRH, which produces preionization before the inductive field is applied. For this reason, a cylindrical-cavity, TE<sub>02</sub>-39GHz gyrotron has been designed by the CRPP and ABB Infocom Ltd., constructed by ABB Infocom Ltd., and installed on the TCA tokamak to study the effectiveness of ECRH-assisted startup.

A flexible ECRH system has been chosen for the TCA tokamak, producing HFS X- or O-mode launching of a gaussian beam in the HE<sub>11</sub> mode. This allows for the study of the relative merit of X/O-mode breakdown scenarios as well as direct X-mode injection from the HFS in HE<sub>11</sub>. The latter has the advantages of high first-pass absorption and a high cut-off density. It permits the prolongation of the initial breakdown pulse, which then allows for current profile control during the initial rampup phase. Efforts will be directed toward the production of well-behaved tokamak discharges with regard to initial current profiles, of runaway-electron content, loop voltage saving, and the general ease of tokamak operation.

The choice of 39GHz was motivated by the value of the toroidal field of TCV. In TCA, the resonance can be placed between  $x=r/a=-0.5$  and  $x=+0.4$ . This allows for the study of upshifted electron-cyclotron current-drive, sawtooth stabilization on both LFS and HFS  $q=1$  surfaces, and reduction in  $m=2$  mode activity possible by properly aiming the beam to produce higher edge power deposition.

### 2. EXPERIMENTAL SYSTEMS

The ECRH system is made up of four main sections: 1) the high-voltage transmission line spanning the 65m between the gyrotron modulator and the gyrotron (located in separate buildings), 2) the gyrotron, 3) the microwave transmission line spanning the 7m between the gyrotron and tokamak, and 4) the microwave launching structure.

#### 2.1 Low-capacitance high-voltage line

A 65m, biaxial, low-capacitance, HV transmission line has been constructed between the HV modulator (10A; -80kV and -54kV) and the triode electron gun (MIG) of the 39GHz gyrotron. The heating current for the gun cathode is supplied by a HV transformer located in the gyrotron SF<sub>6</sub> tank – a solution adopted to avoid the need of placing a third conductor in the transmission line. The transmission line passes through a tunnel with several bends, offering less than 0.6m of free space in some narrow passages.

The line was constructed such that the stored capacitive energy is maintained below the critical crater formation energy of 5J – precluding the use of a dielectrically insulated line. Instead, a large-diameter, non-insulated biaxial line was constructed. The geometry of the two inner conductors, grounded outer conductor, and insulating supports [1] were chosen to reduce the capacitance of the line while maintaining an adequate voltage hold-off. The inner conductors are made of thin-walled SS tubes and the outer conductor of inexpensive commercial ventilation tube, with bends and mechanical connections readily available. Contact between sections was improved to provide good electrical continuity. The result is a line whose maximum stored energy available for arcing is never greater than 4.2J.

\* Vibro-Meter SA, 1701 Fribourg, Switzerland

\*\* ABB Infocom SA, EKR Division, 5401 Baden, Switzerland

\*\*\* Institut für Plasmaforschung, Universität Stuttgart, F.R.Germany

The inherently indeterminate impedance of the biaxial line when arcing occurs, required placement of spark gaps at both ends of the transmission line (along with resistors of average value) to prevent a damaging voltage rise at the modulator or gyrotron. A schematic of the line is shown in Fig. 1. With this protection, uninterrupted pulsing has become routine, demonstrating that such a low-capacitance transmission line can be used when line lengths are not too great. However, since the capacitance is logarithmic with the diameter ratio, merely doubling the length of such a line would require an unreasonably large diameter.

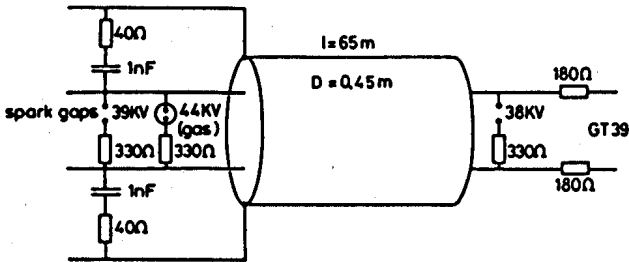


Figure 1. Schematic of high-voltage line.

## 2.2 39GHz Gyrotron

A cylindrical cavity gyrotron was designed to be capable of producing 300kW, 100ms microwave pulses at 39GHz in the TE<sub>021</sub> cavity mode. The maximum efficiency for the design is 42% at full power. The gyrotron uses SF<sub>6</sub> cooling of the MIG and water cooling of the cavity and collector. It fits into the bore of a standard Oxford Instruments superconducting 60/70GHz gyrotron magnet which is operated at reduced field for 39GHz operation.

The gyrotron output is in the TE<sub>02</sub> waveguide mode with a final output diameter of 62.8mm. The gyrotron is connected to a wave number spectrometer [2] via a bellows and a DC break. Unlike the rest of the line these sections could not be laser aligned. For initial in situ testing of the gyrotron, either an octanol-filled microwave load or a small-volume octanol calorimeter was used to terminate the k-spectrometer.

The k-spectrometer was first calibrated for TE<sub>02</sub> at low power (~100mW generated with a Gunn diode) with this calibration later corroborated by calorimetric measurements at higher power (~80kW). The coupling of the k-spectrometer in the TE<sub>02</sub> mode was measured to be -70.5dB. Reflection coefficients of the octanol load and calorimeter used for these calibrations were <0.5% and 4.0%, respectively.

Once mounted in the gyrotron tower, the output

frequency and mode structure of the gyrotron were measured. To avoid measuring stray microwave radiation, the k-spectrometer has been fully shielded with microwave absorbing foam. The perpendicular and parallel k-spectra are shown in Fig. 2. It can be seen that 39.05GHz operation at 80kW provides a clean spectrum with 98% of the output power found in the TE<sub>02</sub> mode. Optimized experimental efficiency for 80kW operation was measured to be 38%. This efficiency is strongly dependent on the applied cavity magnetic field and provides an easy means by which the output power of the gyrotron can be controlled. Gyrotron power levels up to 110kW (non-optimized) at 4.0A have been achieved in the preliminary phase of operation.

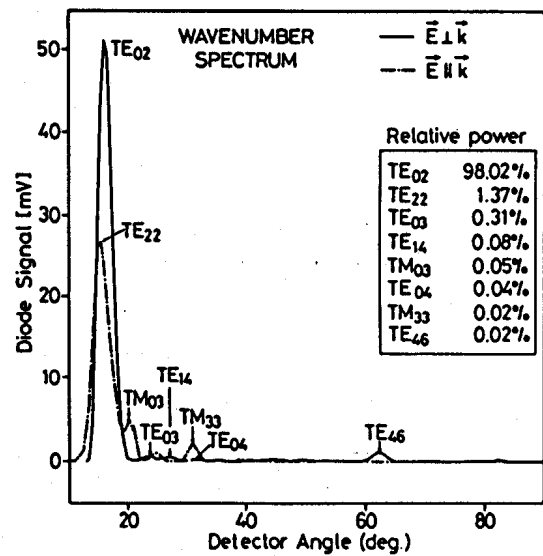


Figure 2. Mode spectrum of GT39 gyrotron.

## 2.3 Microwave transmission line

The TE<sub>02</sub>→TE<sub>01</sub>→TE<sub>11</sub>→HE<sub>11</sub> mode conversion sequence was chosen for the microwave line [3]. Four main restrictions were considered when choosing and placing the individual elements of the line. 1) A measurement of the gyrotron mode structure is required. A k-spectrometer is therefore placed near the gyrotron. 2) The ceiling of the TCA hall limits the height of the vertical portion of the line, requiring a small radius-of-curvature bend at the highest point. In addition, the available floor space roughly fixes the placement of the gyrotron ~7m from TCA. 3) The entrance flange clearance on the TCA vacuum vessel determines the largest possible diameter of the waveguide. 4) Possible vacuum ω<sub>ce</sub> breakdown in the waveguide as it passes to the HFS of TCA requires the placement of the vacuum window at the end of the line, inside the torus.

An overview of the waveguide components in the

line connecting the GT39 gyrotron to TCA is shown in Fig. 3 and Table 1. All of the components were designed and manufactured by IPF Stuttgart, with the exception of the bellows (ABB), and the launching structure (CRPP).

After the TE<sub>02</sub> arc-detector (monitoring the gyrotron window) and the TE<sub>02</sub> DC-break (1KV DC, 5kV for a 10μs pulse), a TE<sub>02</sub> bellows equipped with two Q-band side couplers is placed in the line. The k-

spectrometer is calibrated to provide a TE<sub>02</sub> forward power measurement. An uncalibrated wideband horn (summing both TE and TM modes) yields a reflected power signal used to trip the modulator in the event of a large power reflection.

A reduction of the waveguide ID with the TE<sub>02</sub> downtaper leads to a reasonable-size TE<sub>02</sub> bend which meets the stringent height requirements in the TCA hall.

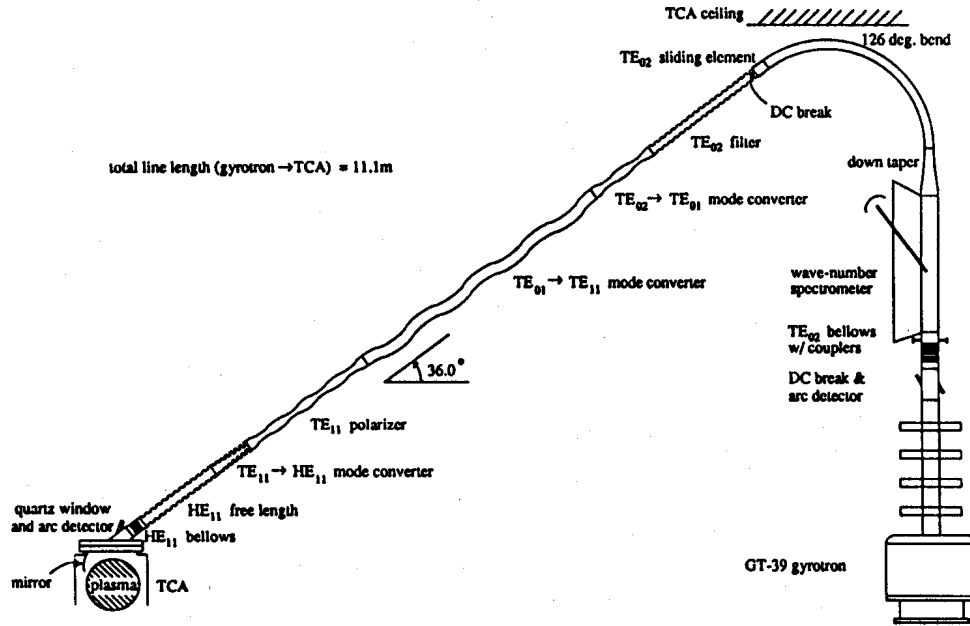


Figure 3. 39GHz microwave line.

Element	Wall-type	Material	Length (mm)	P <sub>ohloss</sub> (%)	P <sub>unw.m</sub> (%)	M-Pur. (%)	Conv-effic. (%)
TE <sub>02</sub> -arc-detect. (62.8mm)	smooth	Cu	120.	-	-	-	-
TE <sub>02</sub> -DC-break	smooth	Cu	120.	-	0.1	99.9	99.9
TE <sub>02</sub> -bellows	smooth, Δr=.415mm	brass, gold-pl	146. ±7.	-	-	-	-
k-spectrometer	smooth	Cu	2000.	0.27	-	-	99.73
TE <sub>02</sub> -down-tap(to 35.2mm)	smooth, non-lin.	el-dep. Cu	440.	0.1	0.01	99.99	99.0
TE <sub>02</sub> -bend 126°,sin-curv.	corrug.[d=0.4(λ/4)]	el-dep. Cu	1924.	0.8	0.1	99.9	99.1
TE <sub>02</sub> -sliding-element	smooth, Δr=.50mm	brass/SS	75. ±4.	-	-	-	-
DC-break	-	kapton	0.5	-	-	-	-
TE <sub>02</sub> -mode-filter	corrug. [0→λ/2]	SS	1176.	2.7[1]	-	-	97.3
TE <sub>02</sub> →TE <sub>01</sub> -mode-conv	rippled-wall[8per.]	Al	579.	0.3	0.2	99.8	99.5
TE <sub>01</sub> →TE <sub>11</sub> -mode-conv	serpentine-type	brass, gold-pl	2266.	0.9	0.5	99.5	98.6
TE <sub>11</sub> -polarizer	distrib. ellipticity	Cu	1160.	0.8	0.2	99.8	99.0
TE <sub>11</sub> →HE <sub>11</sub> -mode-conv	corrug. [λ/2→λ/4]	brass, gold-pl	338.	0.3	0.6	99.4	99.1
HE <sub>11</sub> -free-length	corrugated	Al	702.	-	-	-	-
HE <sub>11</sub> -bellows	corrugated	Brass	124. ±7.	-	0.3	99.7	99.7
HE <sub>11</sub> -arc-detector	corrugated	brass	74.	-	-	-	-
TM <sub>11</sub> +TE <sub>11</sub> -beat-wave el.	smooth	SS	275.6(1λ)	-	-	-	-
Quartz window	3/2 λ waveguide	water-free	5.914	<0.4	0.4 refl	-	>99.2
focus. ellipsoid. mirror[2]	smooth	SS	-	-	-	-	-
calorim./matched-load	-	Cu,SiO <sub>2</sub> ,oct.	-	-	-	-	-

Notes: [1]: Attenuation: TE<sub>11</sub>:TM<sub>11</sub>:TE<sub>02</sub> / 11dB:14dB:0.12dB [2]: reduces beam divergence from 13.4° to 8.5° (e<sup>-2</sup>)

Table 1. Waveguide components of the 39GHz microwave line.

The TE<sub>02</sub> corrugated-wall resistive mode filter attenuates non-axisymmetric modes before the wave enters the series of mode converters. The mode filter also serves to attenuate any reflected power. After the TE<sub>02</sub>→TE<sub>01</sub> conversion, the TE<sub>01</sub>→TE<sub>11</sub> convertor can be used to exchange X- and O-mode orientation, by rotating the convertor together with the following polarizer element. This elliptical polarizer, when independently rotated, can produce any polarization from linear through circular. The wave is finally converted to the gaussian HE<sub>11</sub> mode with the TE<sub>11</sub>→HE<sub>11</sub> converter, which provides pure X- or pure O-mode illumination when linearly polarized. The calculated mode conversion efficiencies and ohmic dissipations for the line elements are listed in Table 1. The final transport section in HE<sub>11</sub>, also acts as an additional mode filter.

In order to pass through the narrow tokamak entrance flange, a section of waveguide of reduced outer diameter is required. This is provided by a smooth section whose length is equal to one TM<sub>11</sub>+TE<sub>11</sub> beat wavelength, thereby maintaining the HE<sub>11</sub> mode. It is this section which determines the ID of 35.2mm for the line.

The placement of the vacuum window, inside the vacuum vessel on the HFS, allows the microwave line to be left at atmospheric pressure (fed from both ends with CO<sub>2</sub> via the arc detectors) to inhibit waveguide  $\omega_{ce}$  breakdown. The  $\omega_{ce}$  resonance can then be displaced between  $x=-0.5$  and  $x=+0.4$  without crossing the window. The thickness of the microwave vacuum window, made of water-free quartz, was chosen to be  $3\lambda_g/2$  to minimize reflections (0.4% calculated), and designed to withstand 300kW, 1s pulses [4].

#### 2.4 Microwave launching system

A smooth stainless-steel ellipsoidal mirror, placed on the top HFS of the TCA vessel, focuses and aims the beam ensuring the best possible localized power deposition close to the tokamak axis (Fig. 4). The mirror can be moved poloidally and toroidally. The toroidal injection angle can be varied 25° to either side of the perpendicular injection angle. The region of the plasma accessible to the beam in the poloidal plane is indicated in Fig. 4, together with raytracing examples. The mirror reduces the beam divergence from 13.4° to 8.5° half width. Shields have been placed on either side of the mirror to reduce deposits on the mirror and the quartz window.

### 3. LINE CONSTRUCTION

The GT39 gyrotron was directly mounted in its final position in the TCA hall for its initial pulse tests. After

the initial tests and calibrations, the first section of microwave line was built, starting from the gyrotron, up to and including the 126° bend. Construction of the 36° portion of the line then began from TCA using a laser and quadrant detector to align each piece as it was mounted. The angular error existing between these two main sections was corrected by slightly adjusting the angle of the 36° portion of the line (introducing 0.3% of unwanted modes at the HE<sub>11</sub> bellows [5]). The length error was then corrected by inserting the TE<sub>02</sub> sliding element shown in Fig. 3. This procedure allowed for closing of the line without a position adjustment of the gyrotron and k-spectrometer assembly.

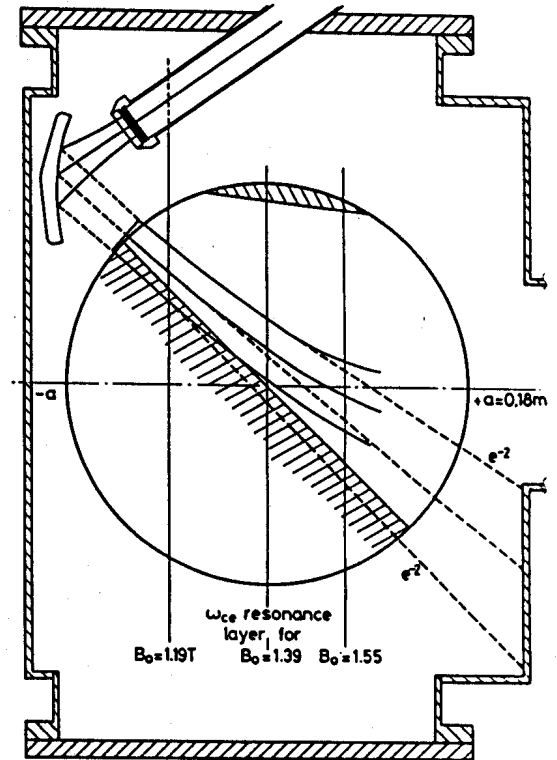


Figure 4. Poloidal plane of TCA. The 39GHz launching structure is shown along with the plasma region accessible to the axis of the beam with perpendicular injection. The ray tracing is performed for  $n_{e0}=10^{19}\text{m}^{-3}$ .

### 4. EXPERIMENTAL RESULTS

The preliminary phase of ECRH-assisted experiments on TCA ( $R/a=.62\text{m}/.18\text{m}$ ,  $B_T=1.55\text{T}$ ) has recently begun. Gyrotron power and pulse lengths have been increased during the short period of operation, to levels which allow for low-voltage operation of the tokamak. Continuous monitoring of the arc detectors and reflected power during this time insured safe operation of the gyrotron and microwave line under all plasma conditions. The TE<sub>02</sub> reflected power measured to be 2% without plasma, reduces typically a factor of 5 during a plasma shot.

Forty kilowatt, 10ms pulses were found to be sufficient to assist the startup of a sustained plasma at loop voltages as low as  $V_L = 1.2V$  ( $\sim 0.3V/m$ ) - a factor of 8 lower than previously possible. Figure 5 shows the initial current rampup for a series of constant- $V_L$  shots. This applied loop voltage is decreased from shot to shot and in each case its value is indicated in the figure. In all cases, the loop voltage is established before ECRH power is applied. The plasma current, consistently starting just after the beginning of the ECRH pulse, is sustained for  $V_L$  greater than 1.2V. For voltages below this critical value, the plasma extinguishes shortly after the removal of the ECRH power. The study of ECRH plasma startup at higher power and longer pulse lengths is planned for the next set of experiments.

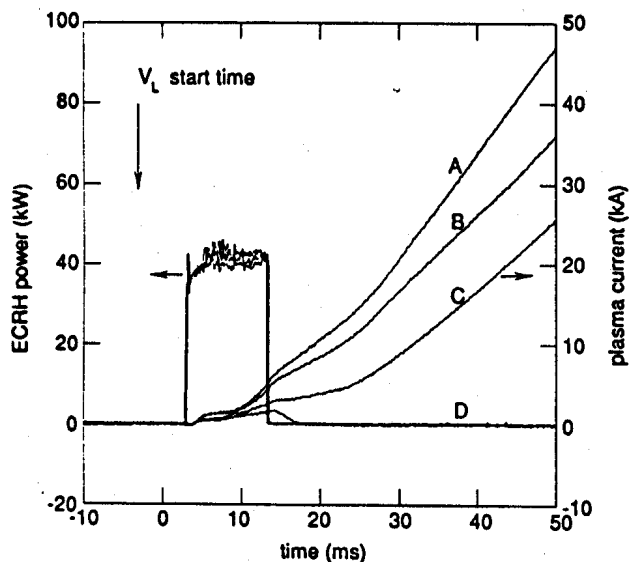


Figure 5. ECRH power and plasma current for applied loop voltages of (A) 1.9V (.49V/m) (B) 1.6V (C) 1.2V (D) 1.0V.

Localized ECRH power deposition was observed using an  $H_\alpha$  camera. The camera, viewing vertically, uses a 128-pixel diode array to provide line-integrated radial profiles of the  $H_\alpha$  emission. The acquisition system acquires one radial profile each 650 $\mu s$  for 40ms, providing a spatially-resolved time history of the  $H_\alpha$  emission during the ECRH startup of the plasma. An example of data taken with this diagnostic is shown in Fig. 6. In this example, the ECRH pulse starts 6ms before the start of the  $V_L$  pulse. Localized ECRH energy absorption is clearly visible before the start of the applied loop voltage ( $V_L$ ). The  $H_\alpha$  profile then becomes that of a standard OH sustained plasma discharge.

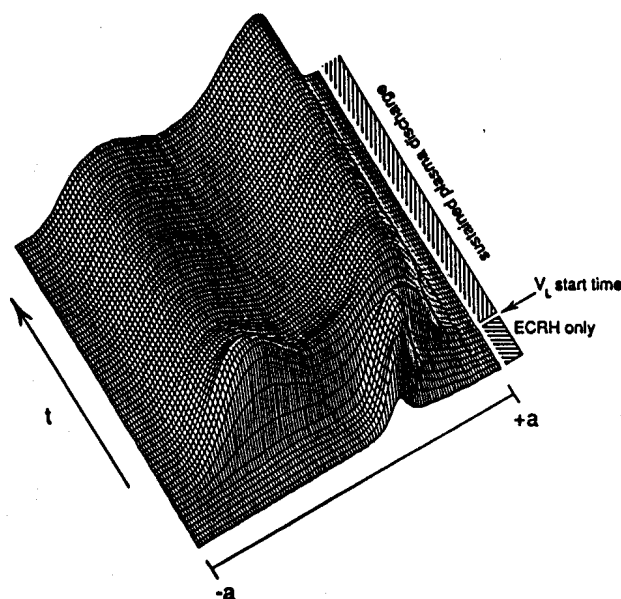


Figure 6.  $H_\alpha$  emission during ECRH-assisted plasma startup. Time duration of plot is 40ms.

## 5. CONCLUSIONS

A 39GHz ECRH system has been designed and installed on TCA. The gyrotron produces a clean mode spectrum with 98% of the output power in the desired  $TE_{02}$  mode. Trouble-free operation of the system has been established, providing reliable transmission of microwave power to the tokamak. Relatively low power (40kW) ECRH startup of the plasma has reduced the electric field required for breakdown to 0.3V/m. Localized power deposition during preionization has been observed.

## ACKNOWLEDGEMENTS

We would like to acknowledge helpful discussions with Dr. A. Cardinali, Dr. A. Knight, and Professor F. Troyon, as well as the support of our colleagues of the gyrotron and TCA teams. We would also like to thank Dr. B. Duval for providing us with his first  $H_\alpha$  camera measurements. This work was partially supported by the Fonds National Suisse de la Recherche Scientifique.

## REFERENCES

- [1] Veneta Isolatori S.R.L., Modell J-9420.
- [2] Kasperek W., and Müller G.A., Int. Journal of Electronics, **64** (1988) 5.
- [3] Thumm M., Ibid., **61** (1986) 1135.
- [4] Dellis A., private communication (1989)
- [5] W. Henle et al. Reports ITER-IL-HD-6-9-E-1/5 (1989).

## DESIGN OF THE TCV TOKAMAK.

G. Tonetti, A. Heym, F. Hofmann, C. Hollenstein, J. Koechli, K. Lahlou, J.B. Lister, Ph. Marmillod, J.M. Mayor, J.C. Magnin, F. Marcus\*, R. Rage

Centre de Recherches en Physique des Plasmas, Association EURATOM - Confédération Suisse.  
Ecole Polytechnique Fédérale de Lausanne, 21 av. des Bains, CH - 1007 Lausanne

Various studies have shown that a significant improvement in tokamak performance can be obtained by elongating and shaping the cross section of the plasma ring. Plasmas with high elongation are however strongly unstable to the vertical axisymmetric mode and their control is a major problem. The objective of TCV (Tokamak à Configuration Variable  $R_0 = 0.88$  m,  $a = 0.24$  m,  $b/a$  up to 3,  $B_{tor} = 1.43$  T,  $I_{plasma}$  up to 1.2 MA) presently under construction at the CRPP is to study scenarios for the creation of such plasmas and to evaluate the improvements in plasma parameters such as the maximum plasma current and density, the confinement time and the maximum pressure that can be sustained.

### 1. INTRODUCTION AND OBJECTIVES.

While tokamak devices have obtained so far the best performances in the direction of controlled fusion, it is already known that a "tokamak reactor" would have an economic interest limited by the maximum pressure that can be confined by a given magnetic field. A limit on the plasma pressure has been observed on all tokamaks which have sufficient additional heating. It manifests itself as a loss in the confinement. A simple scaling law for the maximum pressure has been proposed by F. Troyon (1). It reads :

$$\beta < C \cdot \frac{\mu_0 \cdot I_p}{B_t \cdot a} ; \quad C = 2\% \text{ to } 3\%$$

where  $\beta$  is the ratio of the average plasma pressure to the magnetic field pressure,  $I_p$  the plasma current,  $B_t$  the toroidal field at the plasma center and  $a$  the half width of the plasma in the equatorial plane. This theoretical prediction is now well confirmed by experimental results (2). Tokamaks with circular cross section plasmas have a maximum current limited by the safety factor  $q > 2$  which corresponds to a low  $\beta$  limit of approximately 2%. By elongating the cross section, the maximum current and therefore the maximum  $\beta$  can be increased by a factor of the order of :  $(1 + k^2)/2$  ( $k$  = ratio of the plasma height to width).

This improvement has been recently confirmed experimentally for plasmas with elongations of up to  $k = 2$  (3). Other plasma parameters, such as the density limit and the energy confinement time, are known to scale with the plasma current. Therefore these parameters should also benefit from the elongation. Whether the plasma parameters continue to improve at higher elongation and how they are sensitive to the plasma shape is still a matter of speculation.

An adverse effect of elongating the plasma is the degradation of the global stability which must be compensated for by an active feedback system. The axisymmetric mode (vertical instability of the plasma position) imposes a lower limit on the plasma current as a function of elongation (4). On the other hand, non axisymmetric modes (kink, ballooning) impose an upper limit on the plasma current (5). The stable operating window between these two opposite limits is a function of many parameters such as the value of  $\beta$ , the plasma shape, the plasma wall distance, the current density and pressure profiles. Numerical simulations have been used to demonstrate the existence of scenarios for producing axisymmetrically stable plasmas with elongations up to 3 (6). Whether these plasmas will be stable to the non axisymmetric modes is an open question.

---

\* Present address: JET Joint Undertaking, Abingdon, Oxfordshire OX14 3EA UK



The CRPP has therefore decided to build a versatile tokamak able to produce plasmas with various shapes, including X-point configurations, with an elongation of up to  $k = 3$ .

The objectives of the TCV project are :

- To study scenarios for producing stable elongated plasmas of various shapes.
- To find the scaling of the maximum plasma current, the density limit and the confinement time with the plasma elongation and shape.
- To identify the equilibrium state at high elongation and to determine whether there is an optimal plasma configuration.

Depending on the results obtained, a scheme for the additional heating and possibly current profile control will be chosen to study the  $\beta$ -limit.

## 2. TCV DESIGN and PARAMETERS.

The unusual features of the TCV design result from the large number of poloidal field coils close to the plasma which are required to produce shaped

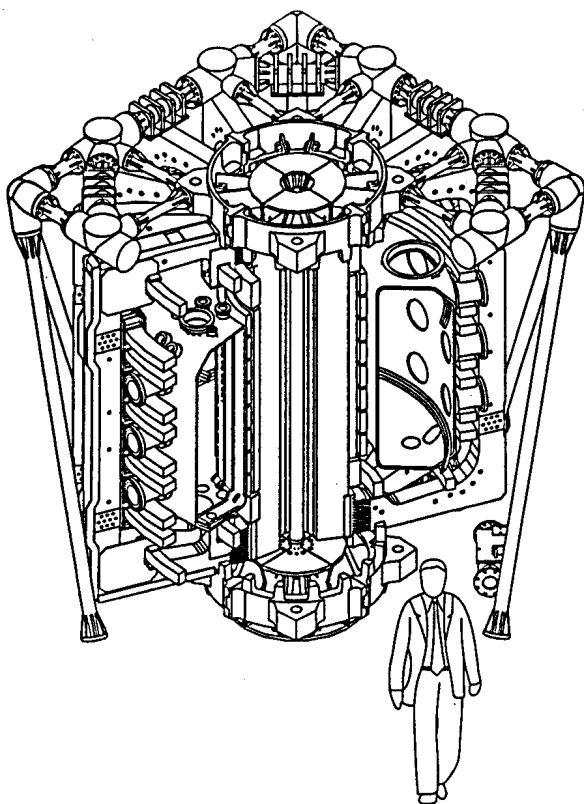


Fig. 1 Configuration of the TCV tokamak

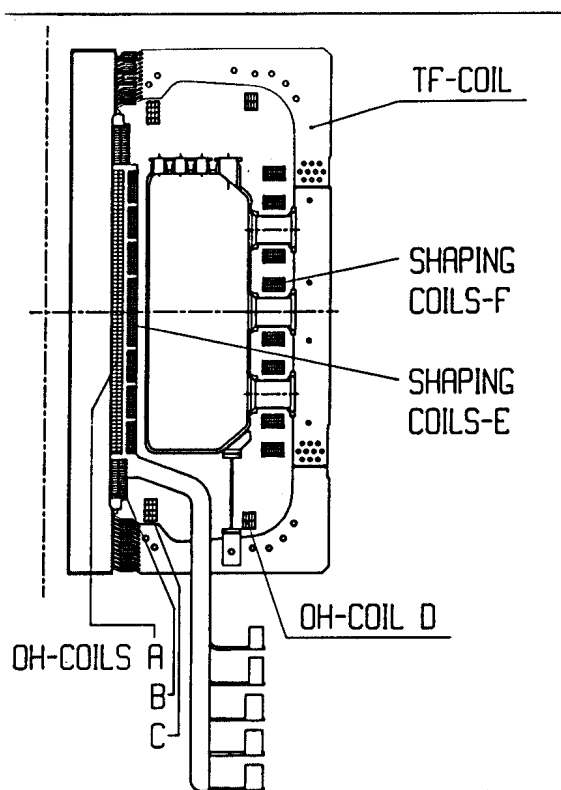


Fig.2 Poloidal cross section of TCV

and elongated plasmas. These coils must therefore be situated inside the toroidal field coils which must be demountable. The OH transformer has no iron core, to avoid further destabilisation of the axisymmetric modes. The most unusual feature is the thick monolithic (i.e. without insulated break) vacuum vessel which results from the physical constraints explained in section 4.

A general view and a poloidal cross section of TCV are shown in Figs. 1 and 2. The main parameters are given in Table 1.

## 3. MAGNETIC FIELD COILS.

### 3.1 Toroidal Field Coils.

The toroidal field is produced by a set of 16 rectangular coils (3x1.45 m o.d.) of 6 turns each. The maximum current is 65 kA giving a field of 1.43 T at the major radius. The turns are machined from 23 mm thick, high strength, high conductivity copper alloy (99.3% Cu, 0.65% Cr, 0.05% Zr). The coil is composed of 4 sections. The inner section is made of wedged plates, with a fibreglass, vacuum

**Table 1. Main parameters of TCV**

Major radius $R_0$	0.88 m
Toroidal field at $R_0$	1.43 T
Flux swing	3.4 ( $\pm 1.7$ ) Wb
Maximum loop voltage	12 V
Plasma width	0.48 m
Maximum plasma height	1.44 m
Maximum elongation	3
Aspect ratio	3.7
Maximum plasma current	
circular, full elongation	250 kA, 1.2 MA
Maximum pulse length	
(Plateau of the current)	1 s
Vessel	
inner dimensions	0.56x1.54m
side wall thickness	15 mm
top/bottom "	20 mm
Vessel time constants	
m=0 , m = 1 modes	13 ms, 8 ms
Vessel resistance	55 $\mu\Omega$
Maximum energy	100 MJ
and power per pulse	177 MVA
Pulse rate	1 per 5 min.
Toroidal field coil	
nb. of turns	96
max. current	65 kA
max. voltage	625 V
OH coil A	
nb. of turns	143
max. current	26 kA
max. voltage	1400 V
OH coil B-C-D (series connected)	
nb. of turns (B,C,D)	29, 12, 8
max. current	26 kA
max. voltage	1400 V
Shaping coils E1-E8	
nb. of turns	34
max. current	7.5 kA
max. voltage	620 V
Shaping coils F1-F8	
nb. of turns	36
max. current	7.5 kA
max. voltage	1240 V

impregnated, electrical insulation. This forms a completely rigid assembly which resists torsional forces about the vertical axis. The horizontal and vertical limbs of the coil are made from 6 plates isolated by epoxy fibreglass sheets without impregnation. They are strengthened by bolts tying the 6 plates together and further strengthened by H steel beams fitted to the outer edge of the coil. The central column and the horizontal limbs are connected by bolted finger joints to ensure the best electrical connection and mechanical strength. The outer limbs are simply bolted together. The inward force acting on the coil is taken up by the vault structure of the central column and the tilting torque is resisted by the machine frame. 3-D stress calculations give a maximum Von Mises stress in the copper of 160 MPa during normal conditions and 220 MPa in fault conditions. The maximum shear stress in the insulation of the central column reaches 16 MPa. The coils are water cooled through tubes inserted into grooves cut on the side of the copper plates. All the copper plates have been machined by Kabelmetal ( Osnabrück W. Germany).

### 3.2 The poloidal field coil system.

The ohmic heating transformer is composed of the main coil A and the series connected coils B, C and D. The 16 E and F coils control the position and the shape of the plasma. A part of the current in the E coils can also be used to increase the available flux swing. Therefore, the A coil and the set B-C-D must be powered separately to annul the stray field of the OH transformer in both cases. The 16 E and F coils have their own independent power supplies which gives the flexibility to produce many plasma configurations.

All the coil windings are made from oxygen - free, half hard copper bars with a water cooling hole in the middle. The windings are insulated with fibreglass tape and vacuum impregnated with an epoxy resin. The poloidal field coils are of two types. The set A-B-E is part of the central column described below. The coils C-D-F are single coils of classical design.

### 3.3 Central column.

The 96 inner plates of the toroidal field coils are assembled into sectors of 6 (one coil) and vacuum impregnated. Then these 16 sectors are assembled and moulded together into a cylindrical column. This column is covered with a sliding layer on top of which the coils A, B and E are wound. The feeding conductors and cooling pipes lie in the space between the A and E coils and are grouped together in a single arm containing all the electrical and water cooling connections. The completely wound central column is then vacuum impregnated to form a rigid assembly.

Large stresses result from the electromagnetic forces and the thermal expansion of the coils. The thermal stresses are minimized by a microprocessor controlled cooling system which reduces the thermal gradients inside and between the coils. The shear stresses in the epoxy fibreglass insulation at the winding ends are reduced to safe values by specially shaped terminations. The central column is manufactured by Asea Brown Boveri AG (Oerlikon Switzerland).

## 4. VACUUM CHAMBER.

The design of the vacuum chamber is based on the following requirements :

- The plasma must be close to the shaping coils.
- The walls must act as a good passive stabiliser for the vertical axisymmetric mode and the plasma wall separation should be about 40 mm.
- The mechanical strength must resist the large forces resulting from disruptions.
- The toroidal electrical resistance must be large enough to keep the induced current in the vessel to a reasonable level.
- The vessel must withstand heating up to 350 °C.

A completely welded structure without an insulated gap was the simplest design option. The vessel is manufactured from 316 LN stainless steel. The side walls are 15 mm thick and the top and bottom 20 mm thick. The top and bottom covers are made from forged pieces and the side walls are formed from rolled steel plates welded into a cylinder. The pre-machined top and the external cylinder are welded together. The inside is

machined to its final size and the diagnostic ports are also machined. This forms the top half of the vessel. The lower half is made in the same manner. These two halves are then welded together and the external dimensions are adjusted to the final size. This manufacturing procedure, devised by De Pretto - Escher & Wyss (Schio/Italy), ensures final tolerances better than  $\pm 2$ mm in diameter in spite of the deformations resulting from the thick welds. Some of the outer diagnostic ports have to be welded after the assembly of the tokamak in order to allow installation of the F shaping coils.

The inside of the vessel is equipped with many rails to fix carbon tiles and measuring coils for the magnetic diagnostics. The thick vessel walls prevent the radial field from the shaping coils from penetrating fast enough to control the most unstable plasmas. Therefore a pair of 3 turn coils, split into 4 sectors, is fitted inside the vessel at the outer corners to improve the speed of the plasma position control.

Four sectors of the vessel are reserved for the limiters which can be placed at different poloidal positions depending on the type of plasma. The top and bottom of the vessel can be equipped with special tiles for X-point discharges.

The outside of the vessel is equipped with gas heating pipes and a Microtherm™ insulating mantel which allow the vessel to be heated to 350 °C. This should provide excellent vacuum conditions and also good conditions for the in-situ wall conditioning by plasma cleaning and deposition techniques.

A large number of ports are necessary for the diagnostic instrumentation to cover the wide range of plasma configurations to be produced. Two man holes allow installation work to be performed inside the vessel. For the magnetic diagnostics, 4 sectors of the vessel are equipped with 38 pick-up coils distributed poloidally (up to 8 sectors can be equipped) and 38 flux loops are fitted on the outside of the vessel.

## 5. PLASMA STARTUP.

The thick TCV vessel makes plasma breakdown more difficult to initiate because of the limited loop

voltage and the large stray field generated by the vessel currents. The stray field is compensated by the 16 shaping coils and a loop voltage of 10 volts should be enough for the breakdown. It is however intended to assist the plasma start up by a 39 GHz ECRH system. Details are presented in Ref. 7

#### 6. PLASMA and MACHINE CONTROL.

The TCV plasma position and shape are controlled by a complex multi-variables feedback system based on a hybrid digital-analogue matrix computer. Details of the plasma control system are given in Ref. 8

The control of the TCV operation is performed by a distributed network of computers which control CAMAC crates for the data acquisition and microprocessors which in turn control all the subsystems in real time. The user interface is based on a commercial control software, VSYSTEM by Vista Control System, and MDS-PLUS. More information can be found in Ref. 9

#### 7. POWER SUPPLIES.

The power for TCV is supplied by a 220 MVA 90-120 Hz 4 pole turbo generator which has been described in Ref. 10. The electrical network and the 19 high power thyristor rectifiers that feed the TCV coils are presented in Ref. 11

#### 8. DIAGNOSTICS.

To fulfill the objectives of TCV, the diagnostics will be strongly oriented toward the identification of the plasma equilibrium. The diagnostics will therefore be interpreted by an inverse equilibrium code based on a powerful magnetic measurement system (also required by the plasma control) supplemented by diagnostics that provide additional global information to improve the reconstruction of the current density profile (such as a multi channel interferometer with Faraday rotation and soft X ray cameras)<sup>(12)</sup>. TCV will also be equipped with a complex Thomson scattering system with a horizontal beam tangent to the plasma inner radius and vertical beams. The horizontal beam is observed from the top which will give radial profiles across the whole plasma. The

vertical beams can be observed from 3 radial ports which give full vertical profiles for most of the plasma configurations. The diagnostics will also include a multi channel bolometer, spectroscopic measurements, soft X ray diode arrays and CCD cameras. Future developments may include a neutral beam charge exchange system.

#### 9. CONCLUSION.

TCV has been designed with original features which would not be easily implemented on larger machines. This experiment will provide the opportunity to explore new domains of tokamak physics which could be relevant for the design of a fusion reactor.

#### REFERENCES.

1. F. Troyon et al. Plasma Phys. 26A (1983) 209.
2. F. Troyon, R. Gruber, Phys Lett. A 110 (1985) 29.
3. J.R. Ferron et al. 17th EPS Conf. on Cont. Fusion and Plasma Heating, part 1 (1990) 371
4. F. Hofmann et al. Proc. of 14th Symp. on Fusion Technology, vol.1, (1986) 687.
5. F. Troyon, Phil. Trans. R. Soc. Lond. A322 (1987) 163-171.
6. F. Marcus et al. Phys. Rev. Lett. 55 (1985) 2289.
7. A. Pochelon et al. A 39 GHz ECRH System for Breakdown Studies on the TCA Tokamak, this volume.
8. P.F. Isoz et al. A Hybrid Matrix Multiplier for Non Circular Plasma Control, this volume.
9. B.M. Marletaz et al. Distributed Control of the TCV Tokamak Using Modular BITBUS Nodes.
10. A. Perez et al. A 220 MVA Turbo Generator for the TCV tokamak Power Supplies, Proc. of 15th Symp. on Fusion Technology, vol2 (1988) 1449.
11. D. Fasel et al. 19 Rectifiers to Supply the Coils of the TCV Tokamak, this volume.
12. F. Hofmann, G. Tonetti, Nucl. Fusion, 28 (1988) 1871.

## DISTRIBUTED CONTROL OF THE TCV TOKAMAK AND MODULAR BITBUS NODES

Jonathan B. LISTER, Philippe MARMILLOD, Pierre F. ISOZ, Ignazio E. PIACENTINI, Blaise MARLETAZ

Centre de Recherches en Physique des Plasmas, Association Euratom - Confédération Suisse, Ecole Polytechnique Fédérale de Lausanne, 21 Av. des Bains, CH-1007 Lausanne - Switzerland

We describe the "Système Intégré de Données" (SID) for the TCV tokamak. We integrate the machine control, plasma control, data acquisition and analysis into one software and hardware network. Most of SID has been bought in. The exceptions are the Plasma Control System and a modular system of programmable controllers which are described in some detail.

### 1. INTRODUCTION

The TCV tokamak<sup>1</sup> requires many computerised functions : plant control, plasma control, data acquisition and data analysis. We have combined these functions into the "Système Intégré de Données" (SID) reflecting the fact that the data must be integrated as first priority, rather than just the hardware. In this way, the data which are generated as one part of SID must be simply available to all other parts. Although SID is conceived as a whole, its component parts, their choice and design are still identifiable and we discuss them in turn in Section 2. All these component parts had the same constraint that SID must be completely implemented with an estimate of 10 man-years. A limited budget furthermore excluded some choices; a target date of 1990 fixed in 1987 precluded others. The rough philosophy was laid out in 1987<sup>2</sup> following which most of the fine details have been modified.

The constraints mentioned forced us to buy in as many components as possible. In fact the late 1980's saw a vast array of useful products on the market, compared with the late 1970's. A final design criterion was to eliminate as many of the weaknesses in the TCA data system, without creating too many new ones. The timescale has also allowed us to test out some of the concepts, equipment and software on TCA, eliminating some surprises and allowing TCV to start with a fully functional SID.

In spite of the intention to buy in as much as possible, 2 major developments were considered necessary. Firstly we have completed the construction of a Plasma Control System<sup>3</sup> and secondly we have

developed a concept of modular BITBUS controllers for TCV, discussed in detail in Section 3.

### 2 THE COMPONENT PARTS

The full SID is shown in schematic form in Fig. 1 for the hardware integration, and Fig. 2 for the data and software integration.

#### 2.1 Computer System

Our previous experience with PDP's and a large available source of software from experimental physics

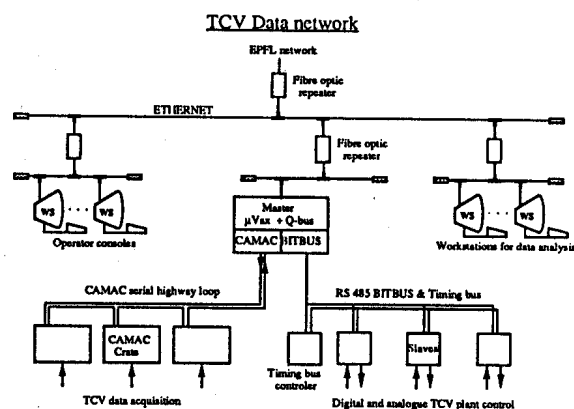


Figure. 1

projects led us to the choice of DEC computers. An initial mix of PDP 11's and microVAXes<sup>2</sup> was quickly replaced by a homogeneous microVAX system for

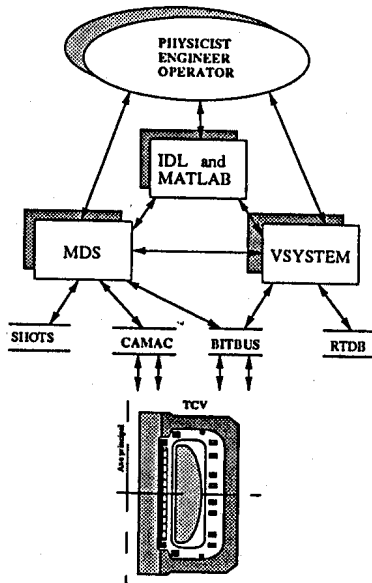


Figure 2.

making full use of available software. Only 3 microVAXes will be equipped with an open Q-BUS, 2 for TCV I/O and one for data storage devices. The remainder will be VAXstations. No large central computer is foreseen, except for the EPFL CRAY. The computers are connected by ETHERNET to the whole network of the EPFL, enabling the connection of our 2 sites over 1 km apart. Within the TCV building, 14 ETHERNET segments are electrically isolated by fiber-optics.

## 2.2 Plant Control

The timescales of tokamak operation separate nicely into slow (asynchronous network, jitter of ~ 0.5 sec) which is adequate for the plant control, and fast (synchronous, jitter of < 1 µsec, hardwired) used for plasma discharge control. Plant control requires 4 components: plant control hardware, a fieldbus, a data store and visualisation software. In a tokamak experiment the plant control hardware is relatively heterogeneous, Section 3. The fieldbus selected was BITBUS which has the following advantages:

- rigidly defined protocol, immune RS485
- fast enough (375 kBaud)
- multi-drop to reduce cabling costs (250 nodes/bus)
- VAX and PC interfaces available
- automatic transmission checking and recovery
- protocol implemented in the INTEL 8044 microcontrollers
- INTEL 8044 firmware is based on a real time kernel supporting up to 7 downloadable tasks and

one standard "Remote Access and Control" (RAC) task.

- some modules are available commercially
- the minimal node is cheap (Sfr 500.-).

Commercial equipment which does not have a BITBUS port (but which may have an RS232C port for example) will be interfaced via BITBUS "translator" modules. 2 years of experience with this fieldbus have convinced us of its choice, and it will soon become an IEEE norm.

The data store and plant visualisation are provided by the commercial VSYSTEM control system toolbox package. This allows us to create live databases across the whole DECNET network and to display the plant state on all our VAXstations for both monitoring and active control. The control desk will be two colour VAXstation 3100/38 computers. Small device handlers must be added to VSYSTEM for customized hardware interfacing. Using this commercial package has reduced the programming effort to a fraction of a person's time. The software runs under X-windows, as will all other parts of SID.

We will have 2 BITBUS fieldbuses, nondedicated, and estimate up to 80 remote modules. We expect up to 10'000 hard- and software channels in the control database.

## 2.3 Timing

Since ETHERNET and BITBUS cannot guarantee the µs jitter necessary for plasma discharge control, we require a separate timing bus. This timing system is distributed throughout the TCV building, and the basic module is described in Section 3.

## 2.4 Plasma control

The Plasma Control System uses a Hybrid Matrix Multiplier<sup>3</sup>, itself controlled by BITBUS. The Plasma Control System will contain over 3'000 12-bit gain settings.

## 2.5 Data acquisition

Data acquisition will be under the MDS+ system<sup>4</sup>. We have installed the previous MDS package to test many of the aspects on the TCA tokamak.

The major source of data will be CAMAC. The lack of intelligence in the CAMAC crates is only rarely a disadvantage. The secondary source of data will be the BITBUS modules, and a third source is the plant control live database. The major volume of CAMAC

modules will be multi-channel ADC's from INCAA, both 16-channel 10 kHz and 4-channel 125 kHz.

The CAMAC crates (20 - 30) will be distributed over the TCV building, connected via 2 Serial Highways using glass fibre-optic cables and with a 5 Mbyte/sec transmission rate. We estimate up to 1500 - 2000 channels for machine and diagnostic acquisition to begin with. The data acquisition rate is therefore quite high, limited by the two microVAXes. The full highway system was supplied by Kinetic Systems International, using the VMS Driver from ORNL.

## 2.6 Analysis

Both MDS+ and VSYSTEM are being interfaced to the IDL and MATLAB symbolic commercial data manipulation and display packages. These two packages have proven to be extremely popular with the physicists and engineers, who no longer program conventionally. In addition to pure analysis, these packages provide the platform for full system integration by building bridges between them and all other data sources.

## 3. MODULAR BITBUS NODES

In spite of an increasing selection of commercially available modules, the specific requirements for tokamak control have forced us to develop a modular hardware solution. We require local intelligent processing of heterogeneous inputs to provide full decentralised control. The BITBUS concept based on a master node and up to 250 slave nodes does not permit inter-node slave-slave communication. For this simple reason we must have a modular BITBUS node to make some measurements and take actions without transiting via the microVAX.

In our modular system, up to seven process input/output cards in single "Eurocard" format can be plugged into a backplane. Addressing via the backplane is performed by a standard processor card controlled by an INTEL 8044 controller, making the whole rack one BITBUS node, Figure 3.

We have added an RS232C UART to the microprocessor board. This port can control an RS232C device, avoiding the requirement for other cards or even a backplane. More importantly, it also allows a standard terminal to take control of the INTEL 8044, allowing us to operate a modular node without a BITBUS connection and without a computer master-node.

## THE MODULAR BITBUS NODE

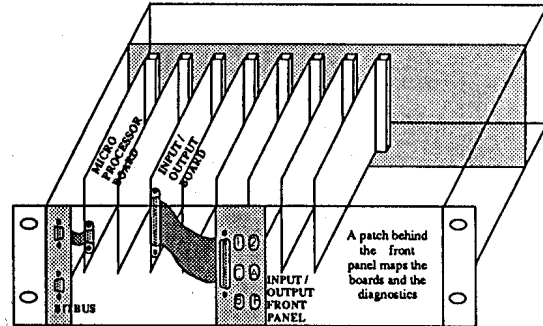


Figure 3.

So far, we have developed 4 I/O cards for the backplane:

- 1) A 24 line PIO card with in addition 3 timer counters for digital I/O and pulse generation,
- 2) A 16 output 12-bit DAC card with internal and external reference voltages, providing both voltage generation and programmable gain amplifiers,
- 3) A 16 input 12-bit ADC card providing cheap and simple data acquisition up to 20 kHz for one channel. Triggering is by BITBUS or externally,
- 4) A 12 channel 16-bit counter-timer. These timing cards are programmable to provide not only a leading edge when triggered by the counter, but can also generate square waves and strobes.

The timing and trigger distribution in a tokamak is almost always developed in-house due to varying opinions about the requirements. We decided that many simple cheap modules fed from a master clock were required and that remote-to-remote timing communication would be limited to a few ( about 5) channels. Our timing system comprises a system-clock running at 1 MHz providing synchronisation. A master clock unit sends out a variable frequency clock train which the remote counters count down to provide local absolute timing. This clock will run for about 3 to 4 seconds at 1kHz, for 23 seconds at 20 kHz providing a resolution during the pulse of 50  $\mu$ sec with a precision better than 1 $\mu$ sec. A third slow period is foreseen after the shot, Figure 4

The timing signals (system clock plus master-clock) are distributed in the TCV Control Bus together with BITBUS, 2 alarm lines and 5 asynchronous trigger lines. This bus comprises a backbone and 15 isolated segments.

## Timing Bus

### RS485 TRANSMISSION

In 25 wires cables normalised on sub D connectors

- 2 LINES BITBUS
- 5 LINES USERS
- 1 LINE MOTHER CLK
- 1 LINE SYNCHRONISATION FOR THE ACQUISITION
- 2 LINES ALARMS
- 2 LINES ELECTRICAL POWER

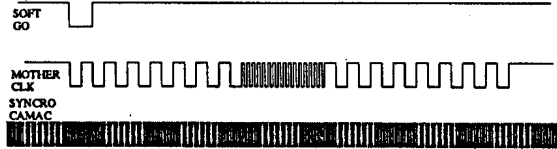


Figure 4.

#### 4. CONCLUSION

By making use of available software and hardware, a relatively small effort can generate a modern tokamak data system.

#### REFERENCES

- 1 G. Tonetti et al., this conference.
- 2 J.B. Lister et al., Internal Report LRP 287/87
- 3 P.F. Isoz et al., this conference.
- 4 MIT, Padova, Los Alamos.

**Acknowledgements :** The authors are grateful for assistance from MIT, Padova, Los Alamos and ORNL.



## A HYBRID MATRIX MULTIPLIER FOR CONTROL OF THE TCV TOKAMAK

Pierre F. ISOZ, Jonathan B. LISTER, Philippe MARMILLOD

Centre de Recherches en Physique des Plasmas, Association Euratom - Confédération Suisse, Ecole Polytechnique Fédérale de Lausanne, 21 Av. des Bains, CH-1007 Lausanne - Switzerland

We have developed a Plasma Control System for TCV based on hybrid analogue digital hardware using DAC-multipliers to produce fast and precise matrix multiplication. The philosophy, construction, performance and cost of this system are described.

### 1. INTRODUCTION

The TCV tokamak under construction at the CRPP has a primary aim of studying highly elongated and shaped cross-section plasmas<sup>1</sup>. In order to provide the necessary shaping flexibility we have 16 poloidal shaping coils and 2 ohmic heating coils to be controlled independently. Since the elongated plasmas are vertically unstable, the Plasma Control System (PCS) must be fast enough to control this unstable mode. Since the highly shaped plasmas will require subtle algorithms to achieve the detailed shapes, the PCS must have the inherent flexibility to control such shapes. Finally, since the PCS will be set up between shots, the system must be simple and easy to use.

The second criterion of flexibility requires that we be able to use a large number of different detection signals, poloidal field probes and poloidal flux loops but also other diagnostics, as the experiment evolves. We consider that over 100 input signals can be usefully combined to control the shape. The PCS will therefore inevitably become large, and will require a large amount of calculation.

Figure 1 shows a schematic of the PCS control loop. We assume 128 raw input signals which must be converted to a reduced number of useable and controllable parameters which have reference inputs for pre-programming. The error signals must then be fed to a dynamic controller which will feed in turn the 18 poloidal power supplies. The strongly coupled shaping coils can be usefully decoupled. Without even discussing the control strategies, we see that there will be many parallel calculations, probably using matrix arithmetic.

Three approaches were considered:

- purely digital,
- a slow part digital and a fast part analogue,
- purely analogue under digital control.

TCV plasma control system

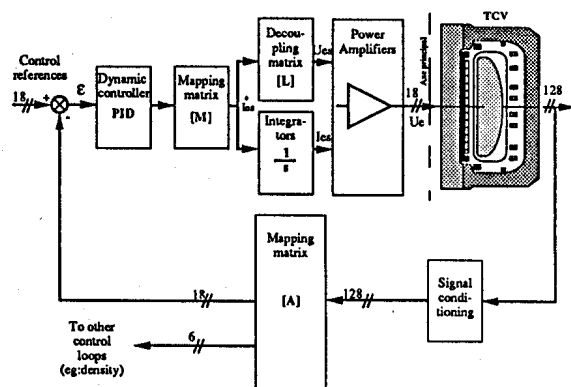


Figure. 1

A purely digital system has a problem of speed if we wish to perform all the control operations with it. It also produces an inherent cycle-time delay which induces undesired phase-shifts in the feedback loop. Its advantage is that it can perform any calculation we should desire, by "simple" re-programming.

The part-digital part-analog system has two disadvantages. Firstly, it requires the development of both approaches. Secondly, it is not obvious, for highly shaped plasmas, that we can so simply choose one fast displacement mode.

The purely analog system under digital control presents a more complex design problem, and is limited to a fixed calculation, mostly sequences of matrix multiplications.

We decided early on<sup>2</sup> to opt for the third solution, restricting the calculations to a large number of matrix operations performed by DAC-multipliers. We have subsequently developed a Hybrid Matrix Multiplier, to be described in the remainder of this paper. This system will be used to control both the C-MOD tokamak (tests late 1990) and the TCV tokamak (tests late 1991).

The PCS must be under computer control for loading the matrix weights. We decided to use the BITBUS fieldbus to communicate between the microVAX computers and the Hybrid Matrix Multiplier, as this is the standard field bus for TCV<sup>3</sup>. The management of the complete system will be implemented under MDS+<sup>4</sup>.

In Section 2 we discuss the modularity and the interconnection philosophy. In Section 3, we present details of the construction of the Hybrid Matrix Multiplier. Section 4 presents the performance of the system. Section 5 discusses the integration into TCV, and finally Section 6 presents some conclusions.

## 2. SYSTEM MODULARITY

The final system must be flexible. The A-Matrix (Fig. 1) has sizes of 96 inputs x 16 outputs (C-MOD) and (128 x 24) (TCV). The controller contains matrices of at least (16 x 16) and (24 x 24) respectively. We may even wish to modify the whole layout in the future to include new control strategies. A suitable modularity was chosen as follows. There is a Base Module (16 x 24). Base Modules can be connected 3 per full 19" crate to make a (48 x 24) matrix. Crates can be connected to make (96 x 24), (128 x 24) matrices and so on. Each Base Module consists of a group of up to 6 Multiplier cards, each performing a (16 x 4) multiplication. Inserting fewer than 6 cards, we can produce smaller matrices, giving (96 x 16) using 6 Base Modules with 4 cards each, as an example. This basic modularity is illustrated in Fig. 2.

Since the final system will have many thousands of weights, considerably attention was paid to the interconnection cabling. The Multiplier cards communicate via analog or digital crate backplane, as do the Base Modules. All analog I/O signals are connected by JET-norm 37-pole 'D'-connectors. Flat

ribbon cable connects the Base Module summer card to its front panel.

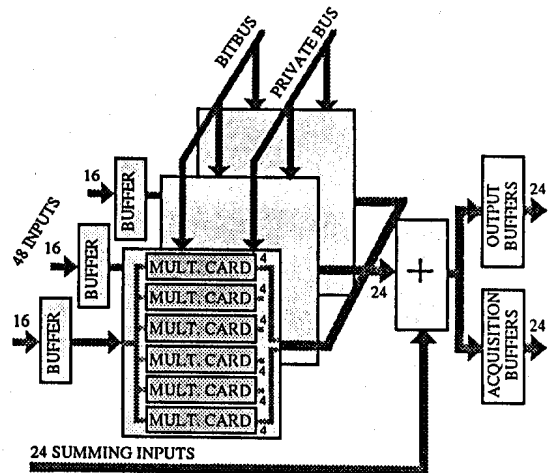


Figure 2. Systeme Modularity

## 3. CONSTRUCTION

### 3.1 Base Cell

The Base Cell is designed around the AD 664 4-quadrant quad DAC-multiplier which can be loaded with a 12-bit digital gain. The analog input signal is applied to the reference input, Fig. 3.

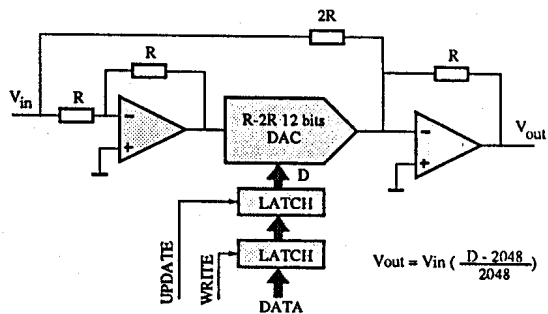


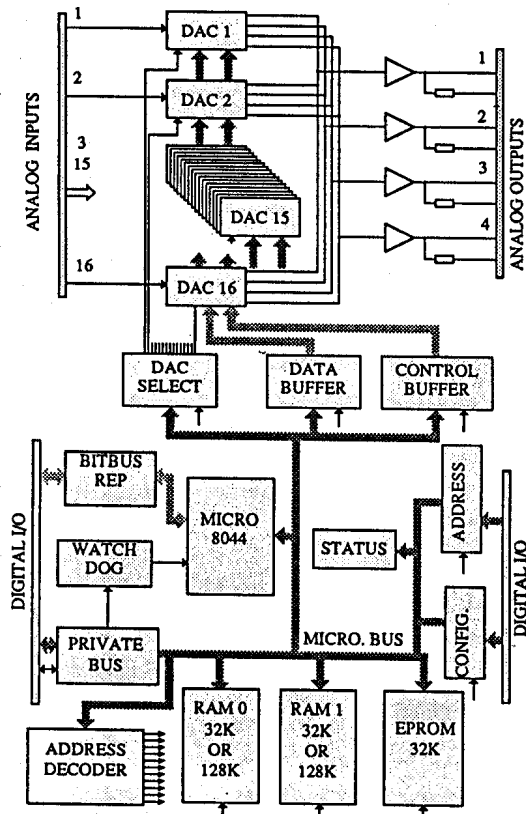
Figure 3. Base Cell

The main drawback of this chip is the high frequency breakthrough at zero gain, leading to an excessive error increasing with the frequency. This problem was modelled and compensated for several test DAC's. We found that the whole batch of DAC's could be adequately compensated using fixed components.

### 3.2 Multiplier Card

The (16 x 4) modularity requires 16 quad DAC's on a double EUROCARD card, Fig. 4. The outputs are summed 16 times. The summing amplifier has a gain of 0.25 to reduce the probability of overflow. The 16 inputs and 4 outputs are obtained from the analog backplane, and sent to a current summing bus on the same backplane respectively. Each digital input is loaded from a latch, given a strobe signal. The latch itself is loaded by software running in an onboard INTEL 8044 microcontroller. This microcontroller is controlled by BITBUS distributed on the digital backplane.

Each Multiplier Card also has its own memory which can contain up to either 490 or 1900 matrices each of size (16 x 4 x 2 bytes) depending on the size of the onboard memory. The Multiplier Cards are therefore autonomous and contain a bank of possible matrices. These must then be loaded into the DAC's themselves under real-time control.



**MULTIPLICATION BOARD DIAGRAM**

Figure 4.

The BITBUS fieldbus unfortunately does not support a broadcast to multiple slave nodes and is too slow for real-time control. We have therefore incorporated a parallel address bus (Private Bus) which is distributed to all the cards in one matrix. The Private Bus defines the slot address of the matrix to be loaded, and each microcontroller then loads its latches with its portion of the full matrix. When all are ready, a strobe causes all the matrix weights to switch simultaneously.

### 3.3 Base Module

The Base Module comprises up to 6 Multiplier Cards feeding up to 24 analogue summing lines. A summing card in the Base Module sums the outputs from up to 3 Base Modules, and also adds in an "external" summing input for chaining crates and for inputting reference signals, perturbation signal or pre-programming signals. If several Base Modules are connected in parallel in a crate, the additional modules have 16 inputs, but no outputs. The connections between the Base Modules are configured with jumpers on the backplanes.

### 3.4 Crate

A 19" Crate houses analogue and digital power supplies, fan-cooling, analogue and digital backplanes and the BITBUS input/output connectors.

## 4. PERFORMANCE

The digital performance is defined by the matrix update rate, measured at on change per 1.3 msec. This is close to the TCV thyristor firing rate and will be more than adequate for both TCV and C-MOD.

The analogue performance is limited by several factors, both DC and AC. The DC errors are:

- output offset, less than one LSB and correctable,
- zero gain breakthrough, up to 30 mV if all 16 inputs are at + 10 Volts,
- zero input, gain = 1.0 gives a non-zero input offset of a few mV.

The AC errors are not limited by the DAC bandwidth, the multiplier cards being filtered at 50 kHz to eliminate switching transients as well as amplifier noise. The AC limitation is a capacitive breakthrough even after compensation, Fig. 5, when the phase also starts to shift. We consider that this performance is going to be more than adequate.

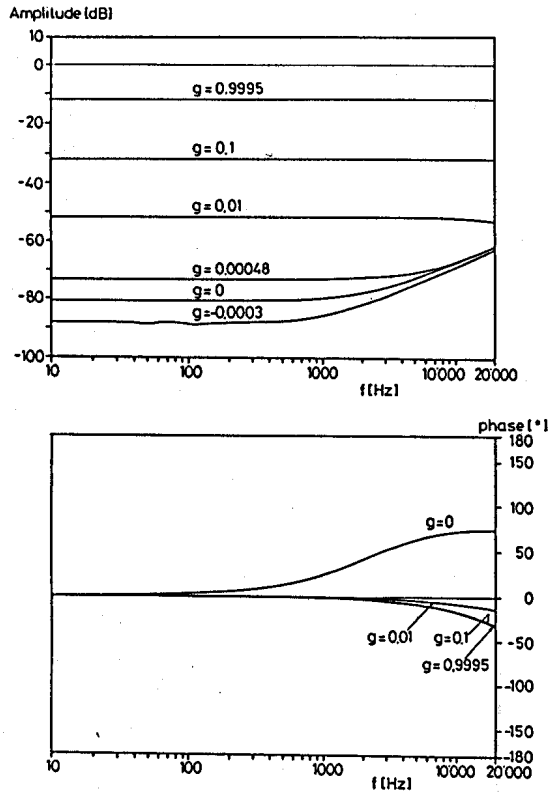


Figure 5. Dynamic Performance

The final performance figure is the time to load new matrices between shots. This is limited by the BITBUS throughput, and we measure a time of 7 msec per matrix per Multiplier Card. Since each card will store many hundreds of matrices, we do not imagine a large loading requirement between most shots.

## 5. INTEGRATION

The analogue performance will be permanently monitored by the MDS+ system during shots and during tests. The matrices themselves will also be managed by MDS+<sup>4</sup>.

The simplicity of the BITBUS communication in the microVAX computers has led us to implement simple operating procedures interactively and in batch-mode via two maths packages, MATLAB and IDL.

During plasma operation there is a Real-Time node controlling each Private Bus. These units are also BITBUS units, programmed according to the experimental requirement.

## 6. DISCUSSION

The development of the full system up to its delivery to C-MOD in September 1990 has taken about 2-man-years. The final construction was mostly subcontracted. The component cost of the full system, including spares, corresponds to about SFr 60.- per matrix weight, of which the quad DAC's themselves account 50%.

The simple incorporation of the microcontroller and its power have contributed to the system flexibility and ease of operation. The simplicity of BITBUS has greatly helped the development of the component parts.

The limitation to matrix arithmetic will still allow many control algorithms, not only piece-wise linear, but also more speculative non-linear mappings for the "A" function<sup>5</sup>.

## Acknowledgements

We wish to thank Martin Greenwald of MIT for many fruitful discussions on the full system. This work was partly supported by the Fonds national suisse de la recherche scientifique.

1. G. Tonetti et al., this conference.
2. J.B. Lister et al. LRP 287/87
3. J.B. Lister et al., this conference.
4. C-MOD team, private communication.
5. J. B. Lister, H. Schnurrenberger, Ph. Marmillod, LRP 398/90.

## 19 RECTIFIERS TO SUPPLY THE COILS OF THE TCV TOKAMAK

D. Fasel, G. Depréville\*\*, A. Favre, J-D. Pahud\*, A. Perez, F. Puchar\*\*

Centre de Recherches en Physique des Plasmas, Association EURATOM - Confédération Suisse  
Ecole Polytechnique Fédérale de Lausanne, 21 av. des Bains, CH - 1007 Lausanne

This paper describes the electrical network designed to supply the 19 coils of the TCV (Tokamak à Configuration Variable) tokamak. After a brief description of the main purpose of TCV, the general characteristics of the TCV network are given. Then the technical choices made for the rectifier power stage are detailed. There follows a description of the rectifier digital control electronics. Comments on simulations carried out and the actual status conclude the paper.

### 1. Introduction

The TCV under construction at the CRPP in Lausanne is designed to study highly elongated plasmas. This objective requires 16 poloïdal coils, designated as shaping coils, placed around the vacuum vessel in order to shape and stabilize the different plasmas, which will

be up-down non-symmetric. Each of them needs its own power supply in order to be driven independently. The coils described above are indexed by the letters E and F. Details on the TCV tokamak structure are presented in [1].

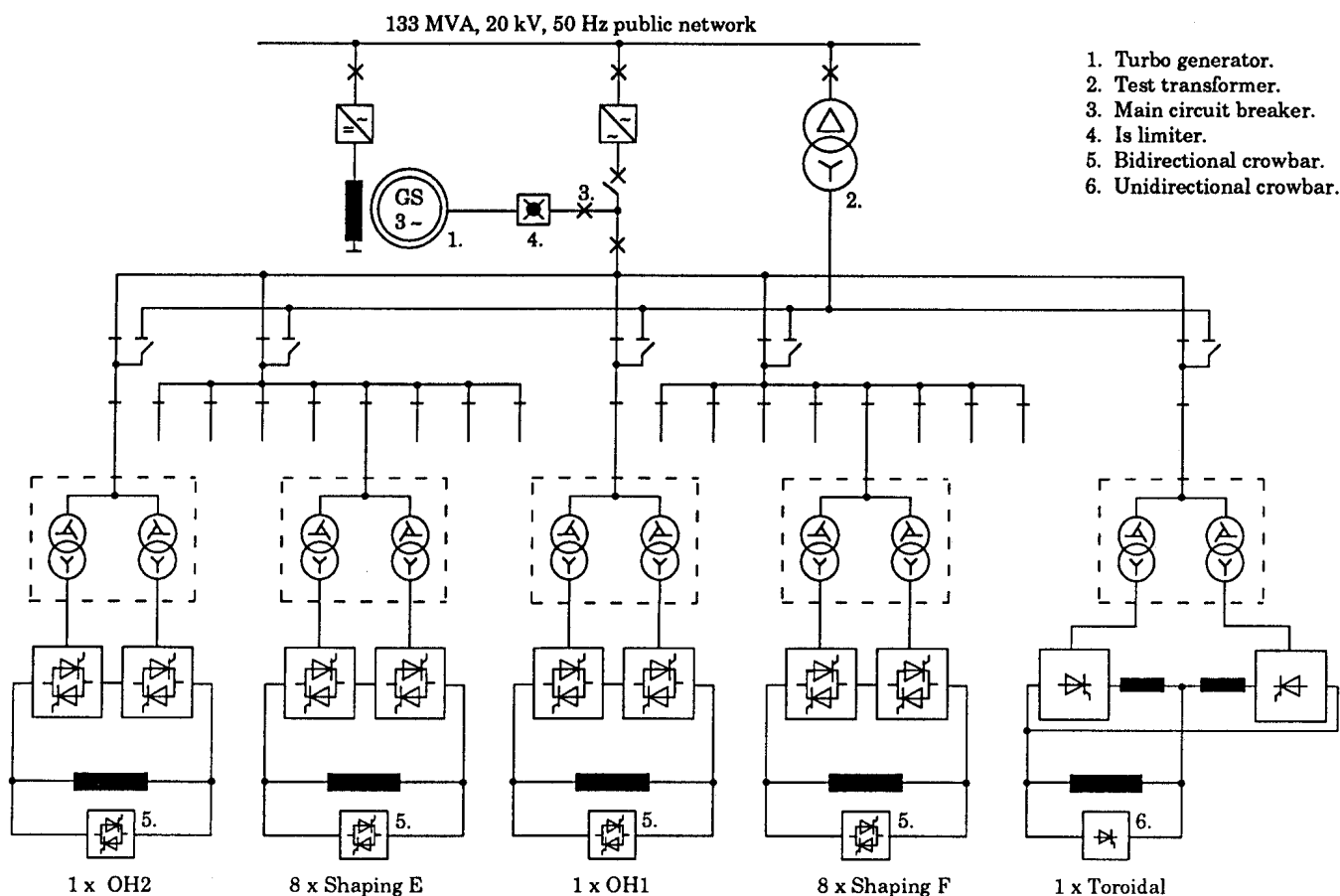


Figure 1: TCV ELECTRICAL NETWORK

\* CERN, SL Division, Geneva, Switzerland

\*\* Jeumont Schneider Industrie, Champagne-s-Seine, France

The A coil, and the B-C-D coils connected in series, induce the ohmic plasma current. They are independently supplied by two rectifiers. The toroidal coil, divided in 16 sectors around the torus, also has its own power supply.

Later we plan to fit fast coils inside the vacuum vessel to stabilize the rapid vertical displacements of the elongated plasmas.

## 2. TCV electrical network

In Figure 1 the TCV power supply network is presented. Two sources are available.

A turbo generator is used as the principal power source, since the regional grid is too weak to supply all the electrical equipment directly. Details of it are given in [2] and only the main characteristics are given below:

Nominal Voltage	10 kV
Nominal Power	220 MVA (4s / 5min)
Short circuit power	1160 MVA (120Hz)
Frequency range	120 to 96 Hz
Stored Energy	347 MJ (at 120 Hz)
Extractable Energy	125 MJ

A main circuit breaker (see n°3, fig.1) allows us to disconnect the power source from the load when severe faults occur, detected either by transformers or rectifiers. If the main circuit breaker is opened due to trip commands coming from other equipment, the rectifier electronics are also informed.

A higher level of protection is achieved with AC phase "Is limiter", (see n°4, fig.1). These are pyrobrowsers, which safeguard the generator from faults occurring on the 10 kV network. They are triggered by the value of the current rate of change before the peak asymmetric current is reached.

The other way planned to supply the TCV network uses a test transformer directly connected to the grid via a circuit breaker. Its characteristics are the following:

Voltage	20 kV / 5.2 kV / 50 Hz
Peak Power (1hour/5h.)	1.9 MVA

This supply will only be used for test purposes. For this, a dummy load formed by four coils from the W VII stellarator (IPP Garching) will be used.

Ten incoming feeder isolators allow us to (dis)connect these two power sources to the five following groups of power supplies: toroidal, ohmic internal and external, shaping internal and external. The toroidal and the two ohmic busbars each have one feeder isolator. The two shaping busbars both have eight feeder isolators.

Three phase cables connect the feeder isolators to the transformer primaries and the transformer secondaries to the rectifiers.

DC coaxial cables in parallel connect the rectifier DC busbar to the TCV coils, except for the toroidal coil which is fed through busbars. The same cables are used to connect the coils to the crowbars. The crowbars protect the TCV coils and the rectifiers from DC overvoltages. They include several thyristors (depending on the rectifier current design) in parallel with the coil, and are triggered locally by an electronic detection or remotely by a command coming from the rectifier electronics.

## 3. Transformers

Each transformer tank contains two separate active parts, including primary and secondary windings. In order to obtain the necessary phase shift of 30 degrees between the two groups of secondary voltages, the primary windings are of the "elongated delta" type. Windings are composed of two parts which have a turn ratio of  $\sqrt{3}$ , and which are connected as presented in figure 2.

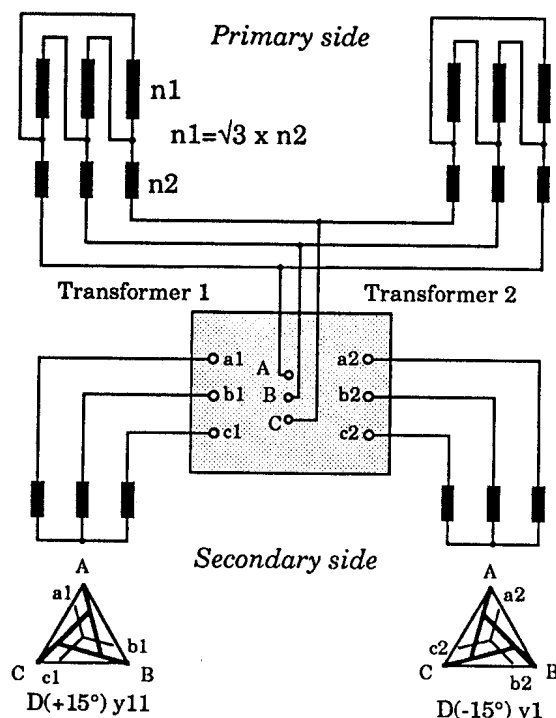


Figure 2 : WINDINGS COUPLING

The active parts of each transformer are identical, only the primary connections differ to obtain the  $\pm 15$  degrees of phase shift, so asymmetries due to manufacturing tolerances are reduced, compared with the usual coupling "delta-Y" and "delta-delta".

A higher short-circuit impedance than usual (21% and 16% at 120 Hz) is needed to minimise the mutual effects of the thyristor commutations from one

rectifier to the others. Table 1 gives the main characteristics of these transformers.

Electrical faults occurring down stream of the transformers will be cleared by the generator main circuit breaker, whose opening time will be less than 200 ms. As a consequence, secondary short circuit type tests have been carried out before delivery, to check agreement with the requirements.

1 x TOR	10 kV/464 V	2 x 25.8 MVA	21%*
2 x OH	10 kV/518 V	2 x 22.8 MVA	21%*
8 x E	10 kV/241 V	2 x 2.6 MVA	16%*
8 x F	10 kV/463 V	2 x 5.1 MVA	16%*

\*at 120 Hz

Table 1 : TRANSFORMER CHARACTERISTICS

All these transformers have been delivered and will be tested on site at the EPFL at 120 Hz, to verify their performance at this frequency.

#### 4. Rectifiers

##### 4.1 Power Section

All the power supplies are based on thyristor semi-conductors, which do not need sophisticated driving hardware and are rapid enough for our application. The generator frequency was designed as high as possible in order to minimise the dead time of the rectifiers. For the same reason, 12-pulse rectifiers are used.

Our first requirement is to use only one type of phase control thyristor for all the rectifiers, with a medium Si plate size (50 mm) and a short  $t_q$  (turn off time) resulting from the use of the higher frequency. These thyristors are assembled in a compact 6-pulse bridge, used as the basic module (3900A-1800V) for the assembled rectifiers, and as a spare device in case of thyristor failure. These bridges are water cooled and include fuses, placed on AC input phases, protecting equipment against thyristor faults.

Each 6-pulse bridge is fed by its own three-phase cable in order to distribute the power losses equally between the thyristors in parallel and to minimise the impedance between the transformers and the rectifiers.

	$U_{dio}$ (V)	$I_d$ (kA)	$n$
1 x TOR	626	78	2 x 10
2 x OH	1400	31	2 x 8
8 x E	651	7.7	2 x 2
8 x F	1250	7.7	2 x 2

$n$  = number of 6-pulse bridges

Table 2: RECTIFIER CHARACTERISTICS

All the rectifiers are 12-pulse power supplies. Table 2 summarises the characteristics of each rectifier type.

The toroidal rectifier consists of two assemblies, each one including ten 6-pulse bridges, connected in

parallel by two air cored reactors. This power supply works only in 2 quadrants.

The ohmic rectifiers consist of two assemblies connected in series, each one including eight 6-pulse bridges. The same is true for the shaping rectifiers with two assemblies, each one including two 6-pulses bridges. All these power supplies work in 4 quadrants, without a circulating current for several reasons: the turns ratio between the ohmic and shaping coils is not large enough to produce an overvoltage due to a zero crossing of the current, the series connection of the assemblies is possible without the use of decoupling coils, the control electronics is simpler and more easily adaptable. The transformers described above are also considerably simplified. With the circulating current at least two separate secondaries would be necessary to feed a 6-pulse assembly.

Each transformer secondary is equipped with an RC + diodes bridge device in order to smooth the AC overvoltage.

These rectifiers will be delivered by Jeumont Schneider Industrie (France), and are now under test in the factory.

##### 4.2 Electronics Section

The design has to take into account several differences between our specific application and the customary practice:

- the working initial frequency
- the decreasing frequency (120 Hz to 96 Hz) during the pulse with a maximum decrease rate of 25 Hz/s.
- important voltage notches created by the thyristor switching in our case in which the generator only feeds power rectifiers.

In addition, the algorithms have to drive the power equipment fed at 50 Hz and at half the nominal voltage, during testing.

Because of the decreasing frequency, it is necessary to adapt the maximum firing angle (inverter condition) during the pulse. Special requirements on the absolute angle accuracy and equidistant pulses are needed to minimise the harmonics on the output voltage, which could disturb the plasma control. The electronics is based on the FDPS (Fully Digital drive Processor System) from Jeumont Schneider Industrie. The multiprocessor structure is presented in Figure 3. Five board types are available, such as:

- Processor board, based on an INTEL 80C196, a 16 bit microcontroller working at 12 MHz and including 12 bits analog I/O. This board is used as a node in the multiprocessor protocol management.

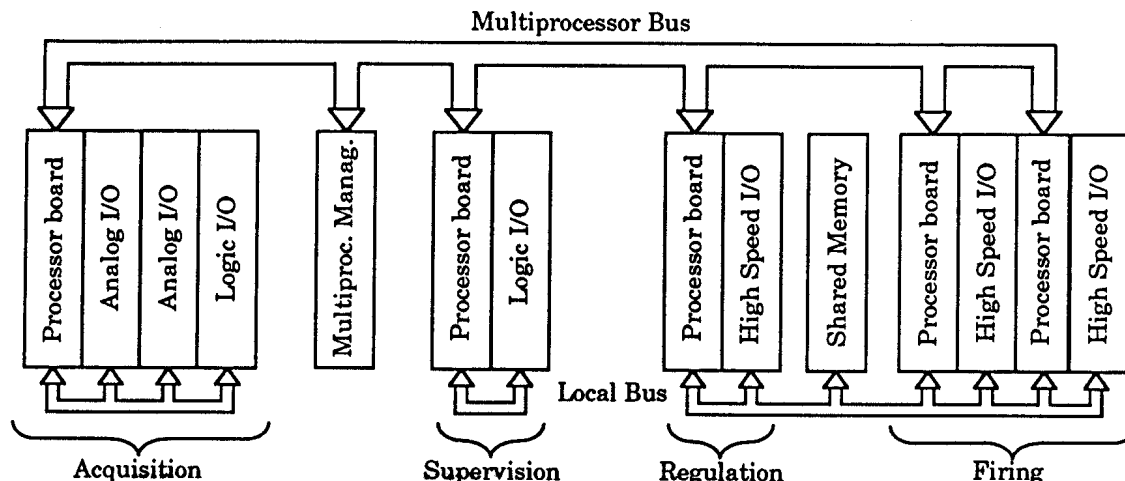


Figure 3 : SCHEMATIC DIAGRAM OF FDPS SYSTEM

- Multiprocessor management board, based on the same processor, used to manage the dialog between the processor boards.

Three types of interrupt level are implemented:

- a highest priority level, activated only if a fault occurs. This starts a specific process including all processors in order to stop the power supplies.
- the second type of interrupt is incident to each processor. It starts the own processor task with a proper sampling period.
- the last interrupt level starts the dialog management between processors.

Each processor is in charge of a particular function: regulation, firing, acquisition, supervision. These are detailed below.

#### 4.3.1 Supervision

A processor is dedicated to the overall supervision of the rectifier. This includes the following functionary processes:

- Alarm and fault sequence management and sending of commands to the other processors.
- Sequences to start cooling, acquisition and rectifiers functioning.
- Management of interrupts level.
- Information exchanges with other processors, which are transferred through the RS 232 link, namely coming from the "TCV control" or locally from the microconsole.

#### 4.3.2 Regulation

Three regulation modes allow us to control these rectifiers. Figure 4 shows three block diagrams corresponding to these different modes.

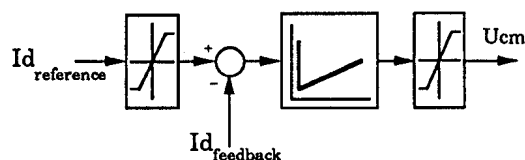
a) **Current feedback** is the usual method of driving the rectifiers. The current is controlled and limited, this mode will be used mainly in tests.

b) **Open loop voltage driving** is used when there is no interest in the precise current value, but in the current derivative. In this case it is necessary to add a current limitation to avoid overcurrent.

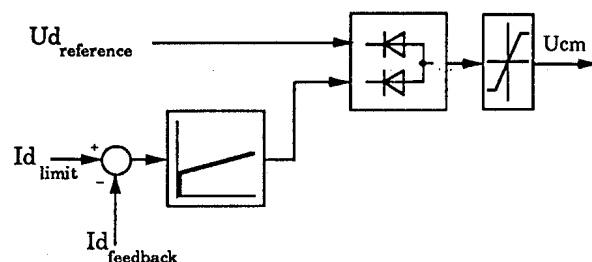
c) **Hybrid mode** is the combination of the two above methods. It allows us to follow a current reference and to do fast current variations around it.

These modes are software selected (see § 4.3.4) and configurable separately for each power supply.

#### a) Current feedback



#### b) Open loop voltage driving (with current limitation)



#### c) Hybrid driving ( a and b )

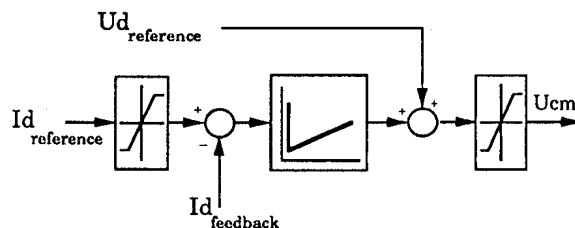


Figure 4 : DRIVING MODES



#### 4.3.3 Firing

The firing processor executes the following tasks:

- reading the new output coming from regulator from the shared memory board.
- firing angle calculation taking into account the current value, the frequency and the commutation notches.
- conversion of firing angle to time and firing pulse generation.
- selection between forward and reverse bridge activation in the case of 4 quadrant power supplies.

#### 4.3.4 Acquisition, control and monitoring

Many signals are necessary to check the correct functioning of the power supplies and analyse faults and alarms quickly. Three types of data are memorised on the rectifier electronics boards:

- continuous data (acquired all the time)
- pulse data (acquired during the pulse)
- fault data (acquired only if a fault occurs)

Between pulses these memorised data are transferred to an industrial IBM PS 2 hard disk. It will then be possible to display the information and/or store it on magnetic tape.

Figure 5 presents the local network allowing the multinode communication (RS 485, 57600 Bd) between the PC (master) and the electronics (slaves).

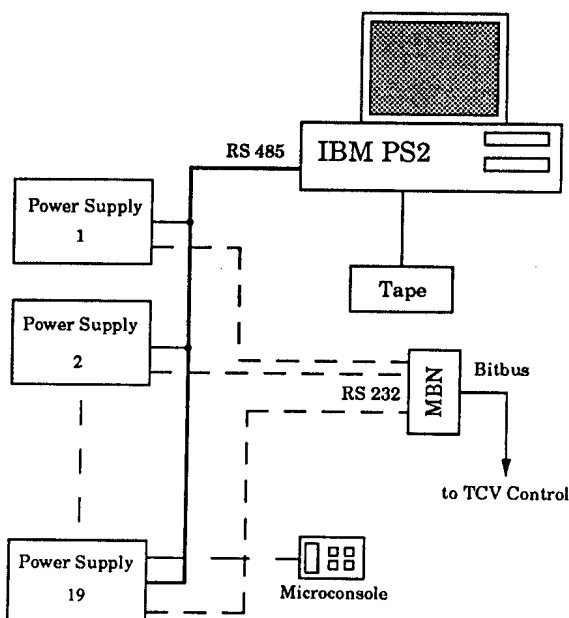


Figure 5 : ELECTRONICS MONITORING

Another function is fulfilled by the PC: the configuration of electronics. Configuration means defining parameters such as: the operation mode (120 Hz or test), the regulation mode, the current limitation

value, the values of the coefficients for the PI/PID regulators and so on. Local modifications of these parameters or reading the alarm and fault stacks is also possible with the microconsole.

"TCV control" gives the main orders and reads the status of the electronics through a bitbus link between a  $\mu$ Vax and a "Modular Bitbus Node", described in [3], which converts the messages, sent through a RS 232 link, into the planned communication protocol.

#### 5. Simulations

In order to confirm calculations, EMTP (ElectroMagnetic Transient Program) is used. This allows us to simulate the complete electrical network, including generator, impedance, transformers, thyristors.... Moreover, we can also simulate the command part namely, the logical signals, trig pulses for thyristors, regulators.

Several simulations have been carried out, as follows:

- Study of the thyristor commutation angle in relation with the value of the absolute limit angle.
- AC and DC short circuit simulations to show the current value reached in different cases: without fuses, using crowbars or driving the thyristors in different ways.
- Influence of the dead time during the zero current crossing.
- Implementation of the three driving modes.

#### 6. Conclusion

The turbo generator and its equipment is functioning. The isolator cells and the transformers are installed. All cables from the turbo generator busbar to the transformer primaries are installed, and the others are delivered. The rectifiers are under test in the factory, after that they will be delivered and tested on site to confirm their performance at 120 Hz.

- [1] G. Tonetti, Design of the TCV tokamak, this volume.
- [2] A. Perez, A 220 MVA turbo generator for the TCV tokamak power supplies, in: Proc. of 15th Symp. on Fusion Technology, vol.2, 1988, p. 1449-1453
- [3] B. Marletaz, Distributed Control of the TCV tokamak using Modular Bitbus Nodes, this volume.